

Geologica Acta: an international earth science journal

ISSN: 1695-6133 geologica-acta@ija.csic.es Universitat de Barcelona España

Pérez-Rivarés, F. J.; Garcés, M.; Arenas, C.; Pardo, G.

Magnetostratigraphy of the Miocene continental deposits of the Montes de Castejón (central Ebro basin, Spain): geochronological and paleoenvironmental implications

Geologica Acta: an international earth science journal, vol. 2, núm. 3, 2004, pp. 221-234

Universitat de Barcelona

Barcelona, España

Available in: http://www.redalyc.org/articulo.oa?id=50520304



Complete issue

More information about this article

Journal's homepage in redalyc.org



Scientific Information System

Network of Scientific Journals from Latin America, the Caribbean, Spain and Portugal Non-profit academic project, developed under the open access initiative



Magnetostratigraphy of the Miocene continental deposits of the Montes de Castejón (central Ebro basin, Spain): geochronological and paleoenvironmental implications

F.J. PÉREZ-RIVARÉS $^{|1|}$ M. GARCÉS $^{|2|}$ C. ARENAS $^{|1|}$ and G. PARDO $^{|1|}$

| 1 | Departamento de Ciencias de la Tierra, Facultad de Ciencias, Universidad de Zaragoza Pedro Cerbuna 12, 50009 Zaragoza. Pérez-Rivarés E-mail: perezriv@unizar.es

|2| Grupo de Geodinámica y Análisis de Cuencas. Dept. Estratigrafia, Paleontologia i G.M., Facultat de Geologia, Universitat de Barcelona

c/ Martí i Franquès, s/n, 08028 Barcelona. E-mail: garces@ub.edu



A detailed magnetostratigraphic study has been carried out in the early to middle Miocene distal alluvial and lacustrine sediments of the Montes de Castejón (central Ebro Basin). The study was based on the analysis of 196 magnetostratigraphic sites sampled along a stratigraphic interval of about 240 meters. Local magnetostratigraphy yielded a sequence of 12 magnetozones (6 normal and 6 reverse) which could be correlated with the Geomagnetic Polarity Time Scale (GPTS) interval C5Cr to C5AD (between 17 and 14.3 Ma.). The sampled sedimentary sequences include the boundary between two tectosedimentary units (TSU, T5 and T6) already defined in the Ebro Basin. The magnetostratigraphy of the Montes de Castejón allows to date the T5/T6 TSU boundary at 16.14 Ma, within chron C5Cn.1n. This magnetostratigraphy also allows us to analyse in detail as well as to discuss the variations in sedimentation rates through space and time between different lacustrine environments: Outer carbonate lacustrine fringes and distal alluvial plains (Montes de Castejón sections) show higher sedimentation rates than offshore lacustrine areas (San Caprasio section, 50 km east of Montes de Castejón).

KEYWORDS | Magnetostratigraphy. Geochronology. Sedimentation rates. Miocene. Ebro basin.

INTRODUCTION

The development of a precise stratigraphic framework in continental basins is often problematic because of the scarcity of absolute chronological constrains, as well as the absence of reliable chronostratigraphic markers. In foreland basins in particular, lithostratigraphic units generally have diachronous boundaries, rapid lateral facies transitions are frequent and, therefore, basin-wide stratigraphic correlations are usually

too uncertain for high resolution basin-scale paleoenvironmental studies. The Tertiary sedimentary record of the Ebro Basin has been studied by many authors from a stratigraphic and sedimentologic point of view in order to decipher its paleogeographic evolution. As a result, many lithostratigraphic units have been named (Riba et al., 1983; Villena et al., 1992). From a genetic point of view, the sedimentary record has been divided into eight Tecto-Sedimentary Units (TSU, see concepts in Pardo et al., 1989) named T1 to T8 (Villena et al.,

1992, 1996; Alonso-Zarza et al., 2002), the ages of which were determined either from mammal biochronology or by correlation with marine equivalents towards the eastern end of the basin. More recent magnetostratigraphic studies have provided further time constraints to some Eocene to Miocene continental successions in the central and eastern parts of the basin (Gomis et al., 1997; Barberà et al., 2001; Pérez Rivarés et al., 2002). These studies combined represent a very long continuous record of approximately 22 Ma, from late Eocene to middle Miocene, and provide a very firm high-resolution chronological framework. Its correlation with the time scale is well supported by mammal biostratigraphic data in the Oligocene sequences and a radiometric age in the lower Miocene sediments of the central part of the basin (Odin et al., 1997). From these studies absolute ages for some TSU boundaries could be determined.

In this paper we present new magnetostratigraphic results from the Montes de Castejón, in the central part of the Ebro basin, which lacks chronological evidence, except for that derived from stratigraphic correlation with the Sierra de Alcubierre (Arenas, 1993; Arenas and Pardo, 1999, 2000), based solely on the tectosedimentary analysis. The aims of this contribution are: 1) to check the previous stratigraphic correlation of the Montes de Castejón units with nearby areas (i.e., Sierra de Alcubierre), 2) to better define the age of the TSU boundaries, and 3) to discuss the varying sediment accumulation rates at particular time intervals and its paleoenvironmental significance.

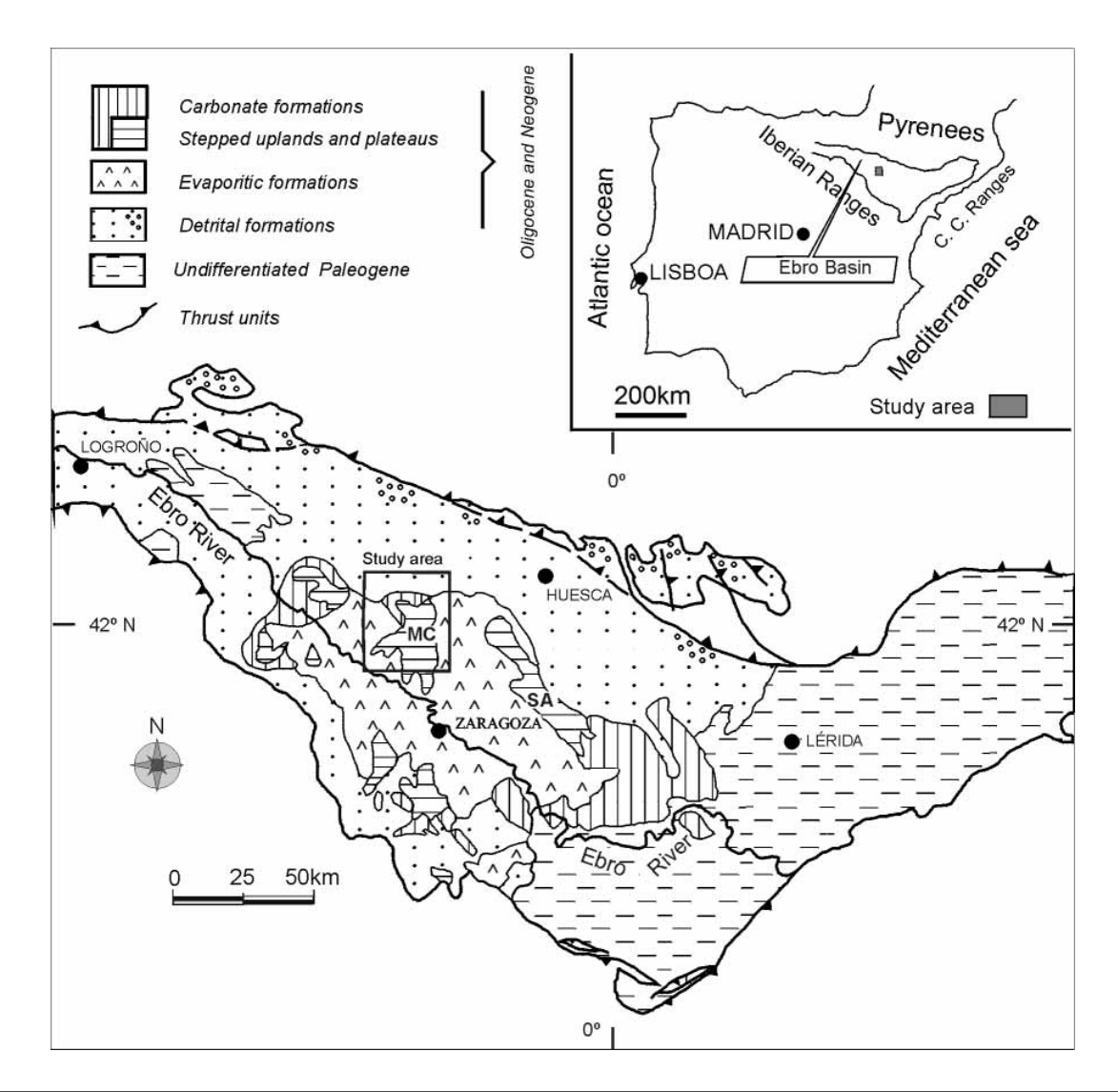


FIGURE 1 Geological map and location of the Ebro Basin and the study area in the Iberian Peninsula (modified from Instituto Tecnológico y Geominero de España, 1995). MC: Montes de Castejón; SA: Sierra de Alcubierre.

GEOLOGICAL CONTEXT OF THE CENTRAL PART OF THE BASIN

The Ebro Basin is one of the largest Tertiary basins in the Iberian Peninsula, generated during the Paleogene as a result of the collision of the Iberian and Eurasian plates. It is bounded by the Pyrenean Range to the north, the Iberian Ranges to the south and the Catalan Coastal Ranges to the east. In the latest Eocene the Ebro Basin became fully continental (Riba et al., 1983) and accumulated up to 5.5 km of alluvial and lacustrine sediments until the middle-late Miocene, when the basin opened towards the Mediterranean sea (Vázquez-Urbez et al., 2003; García-Castellanos et al., 2003). The Oligocene and Miocene record of the central part of the basin consist of coarse to fine detrital sediments deposited in alluvial and fluvial systems originated from the basin margins, and carbonate and evaporite sediments formed in lacustrine systems in the centre.

The studied area (Fig. 1) is located in the central part of the Ebro Basin and was directly linked to the Pyrenean Range evolution (Arenas, 1993; Arenas and Pardo, 2000). In this area, the detrital deposits to the north (Uncastillo Formation, Soler and Puigdefàbregas, 1970) consist of ochre and red mudstones with sheet-and-channel-like, fine to medium sandstone intercalations. These deposits belong to the distal sector of the "Luna fluvial system" (Hirst and Nichols, 1986) and grade laterally southward into lacustrine carbonate and evaporite deposits of the Alcubierre and Zaragoza Formations (Quirantes, 1978), respectively. The Zaragoza Formation is mainly made of nodular gypsum and marls with limestone intercalations that crop out extensively on the southwestern and southeastern sides of the Montes de Castejón. The Alcubierre Formation consists of limestones and marls with scarce fine siliciclastic intercalations. It makes the present carbonate uplands of the centre of the basin, one of which is the Montes de Castejón plateau (Fig. 1). It grades lateral-

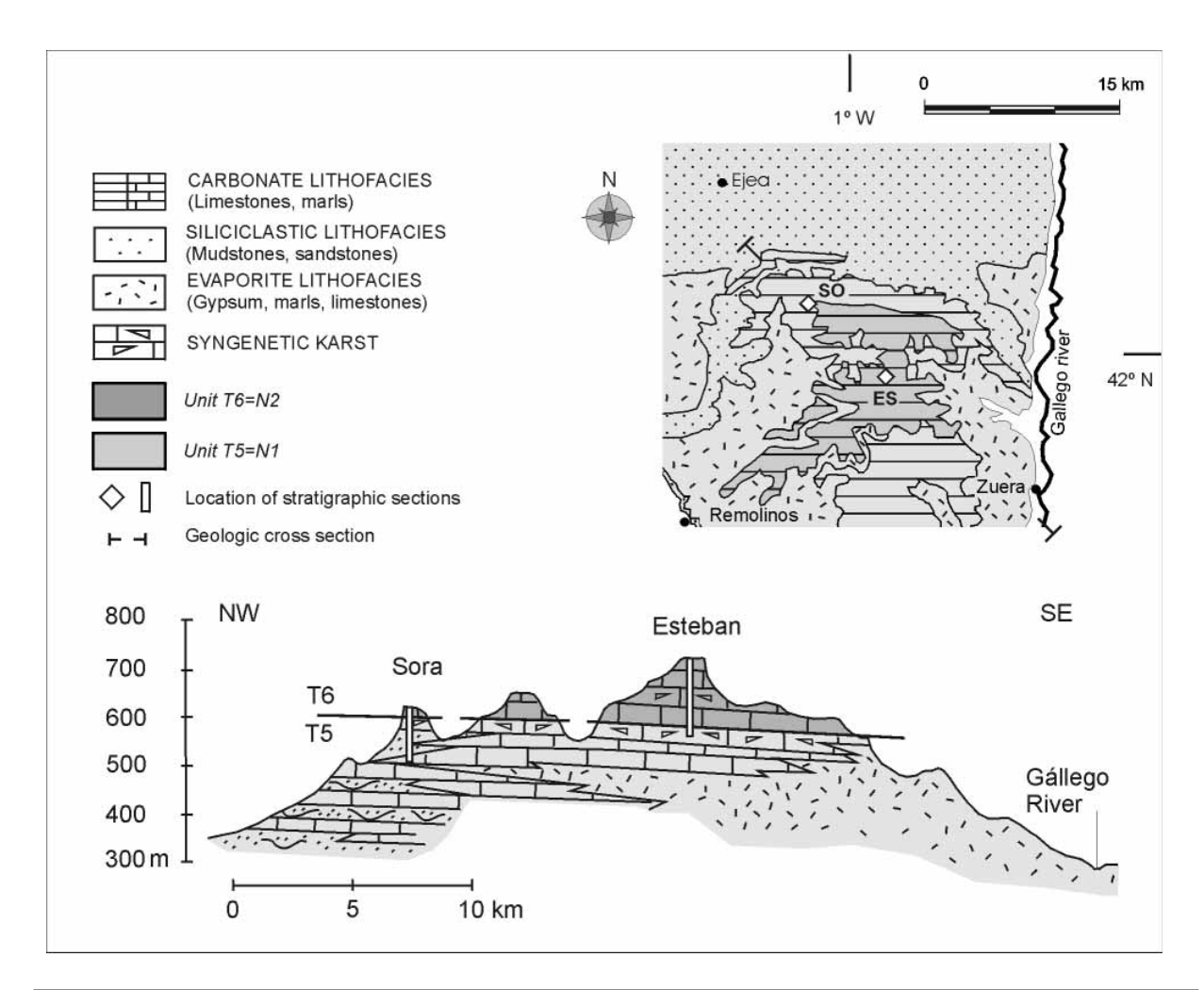


FIGURE 2 | Simplified cartographic map (modified from Arenas, 1993) and geological cross-section of the study area.

ly and overlies the evaporitic deposits of the Zaragoza Formation.

The outcropping succession in the Montes de Castejón lies nearly undeformed, and strata are horizontal or show dips up to 5° southeast. It has been divided into two local TSUs (Fig. 2) with a general but complex, finingupward evolution (Arenas, 1993): the first one (N1) crops out in the lowest parts of the Montes and corresponds to the Uncastillo, Zaragoza and Alcubierre Formations. The second one (N2), which has not any known equivalent deposits in the Pyrenean area, occupies the highest parts of the Montes de Castejón and corresponds entirely to the Alcubierre Formation.

The boundaries between units are sedimentary breaks (in the sense of Pardo et al., 1989) represented by sharp shifts in the sequential evolution. In the southern part of the studied area, evaporite deposits of unit N1 are sharply overlain by carbonate facies of unit N2 (Fig. 2). In contrast, in the northern part, the same boundary is found within a carbonate succession and is marked by the presence of syngenetic karst facies (Arenas et al., 1999).

The lack of chronological data in the Montes de Castejón, along with their disconnection from other areas in the central Ebro Basin, make difficult a chronostratigraphic correlation. Thus, the correlation of local units N1 and N2 with other areas in the Ebro Basin (e.g., Sierra de Alcubierre, 50 km east of Montes de Castejón) was exclusively made by photogeology and similarity of the sequential evolution of the TSU units, resulting in the following: N1=T5 and N2=T6 (Fig. 3). According to Alonso-Zarza et al. (2002) the age of T5 is Agenian (MN2)early Aragonian (MN4) and the age of T6 is middle Aragonian (MN4)-late Aragonian (MN6). These ages were not very accurate because were based on very few fossil sites whose biochronological assignment has been object to several revisons (e.g., the Villanueva de Huerva site, Pérez et al., 1985; Cuenca et al., 1992). Recent magnetostratigraphic studies by Pérez-Rivarés et al. (2002) in the Miocene deposits of the neighbouring Sierra de Alcubierre provided a reliable absolute chronology for some of the younger TSU boundaries: T4/T5 21.2 Ma, T5/T6 16.4 Ma and T6/T7 14.4 Ma.

From a sedimentological and paleogeographical point of view, sediments corresponding to units T5 and T6 represent a lacustrine system that extended throughout the central part of the Ebro Basin during the early and middle Miocene. Good examples of this lacustrine environment are described in the areas of Sierra de Alcubierre and Montes de Castejón. Cyclic water level changes in the lake system resulted in alternating carbonate facies, at times of high water level, and evaporite facies, at times of low water levels. Periods of highstand lake level were charac-

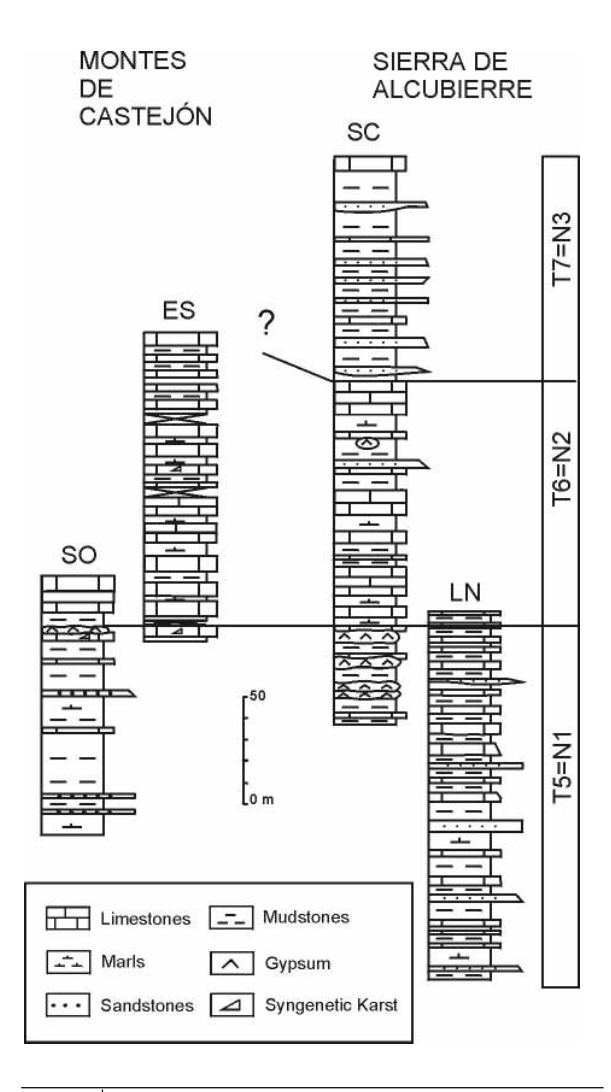


FIGURE 3 Stratigraphic correlation of some sections in the Montes de Castejón and Sierra de Alcubierre areas according to Arenas (1993) and Arenas and Pardo (2000), with indication of equivalent nomenclature of TSU (Tectosedimentary units). SO: Castillo de Sora; ES: Esteban; SC: San Caprasio; LN: Lanaja.

terised by a maximum extent of a unique water body, while lowstands could correspond to several isolated sulphate depositional areas (Arenas and Pardo, 1999). These sulphate areas in some cases (e.g. unit T5 in Montes de Castejón) were separated through low-relief subaerial barriers that experienced saline diagenetic processes during low lake levels and dissolution-precipitation processes in subsequent water level rises; these correspond to the syngenetic karst zones (Arenas et al., 1999).

STRATIGRAPHIC SECTIONS

For the purpose of this contribution, two stratigraphic sections that cover the entire succession of the Montes de Castejón were chosen for paleomagnetic analysis (see Fig.

2 for location): the Castillo de Sora section in the northwestern part, and the Esteban section in the northern central part. See Arenas (1993) and Arenas et al. (1999) for details.

The Castillo de Sora section (Fig. 4) has a total thickness of 118 m and it has been divided into four parts. From base to top, the first one consists of grey, green, ochre and reddish mudstones and marls with mostly brown and grey sheet-like, fine sandstone intercalations. Sandstones have horizontal and cross lamination, ripples and may have sulphate cement. At places, mudstones contain scattered gypsum nodules. At the base and top this interval contains some thin grey and beige, mostly bioturbated, bioclastic limestones. The second part is made of mostly reddish and ochre mudstones and minor grey marls with thin, grey bioclastic limestone intercalations and some fine ochre and grey sheet-like sandstone layers. Scattered gypsum nodules can be present in some reddish mudstones. The third part consists of alternating grey marls and thin beige, yellow

and grey limestones with nodular gypsum, either as continuous layers or scattered nodules. Limestones associated with gypsum are horizontally laminated (micrite, at places dolomicrite, with very thin, fine sandstone and silt laminae and lenticules) and contain some gypsum nodules, breccia and dissolution facies (e.g., syngenetic karst facies). The boundary between units T5 and T6 is located at the top of those levels. The fourth part of the section shows thick strata of beige limestones with beige and grey marl intercalations. At the base, limestones are mostly laminated as those described above, while toward the top of this part bioclastic limestones, at places bioturbated, are dominant.

The Esteban section (Fig. 5) has a total thickness of 141 m and has been divided into three parts. From base to top, the first one consists of beige and yellow laminated limestones and dolostones and beige, brown and grey marls. Carbonate layers contain cavities, cracks, silica nodules and layers, and evaporite nodules and pseudomorphs.

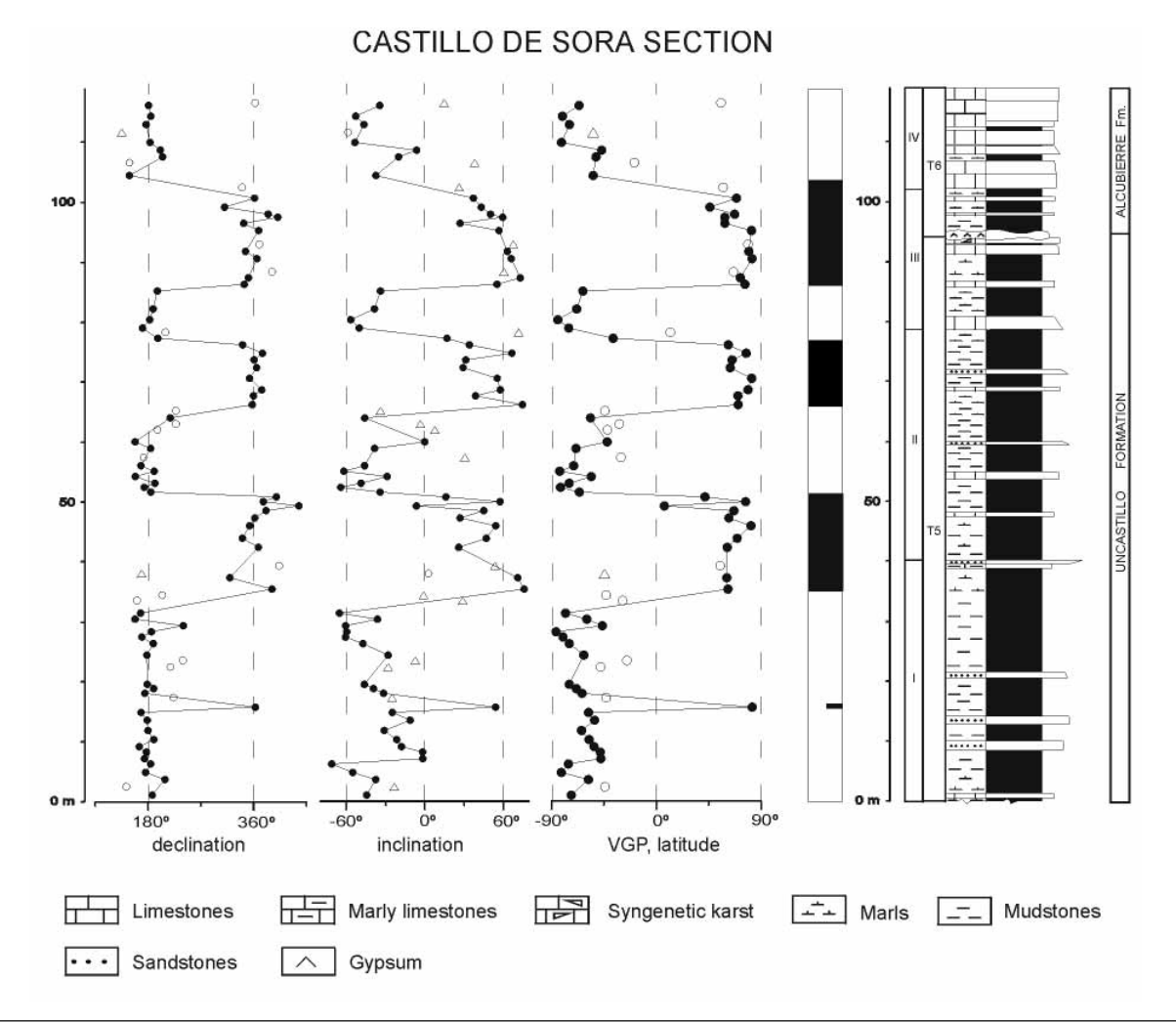


FIGURE 4 Stratigraphic column and magnetostratigraphy of the Castillo de Sora section. Solid dots represent highly reliable directions, open circles and triangles represent less reliable ones. Black (white) bands represent normal (reverse) polarity.

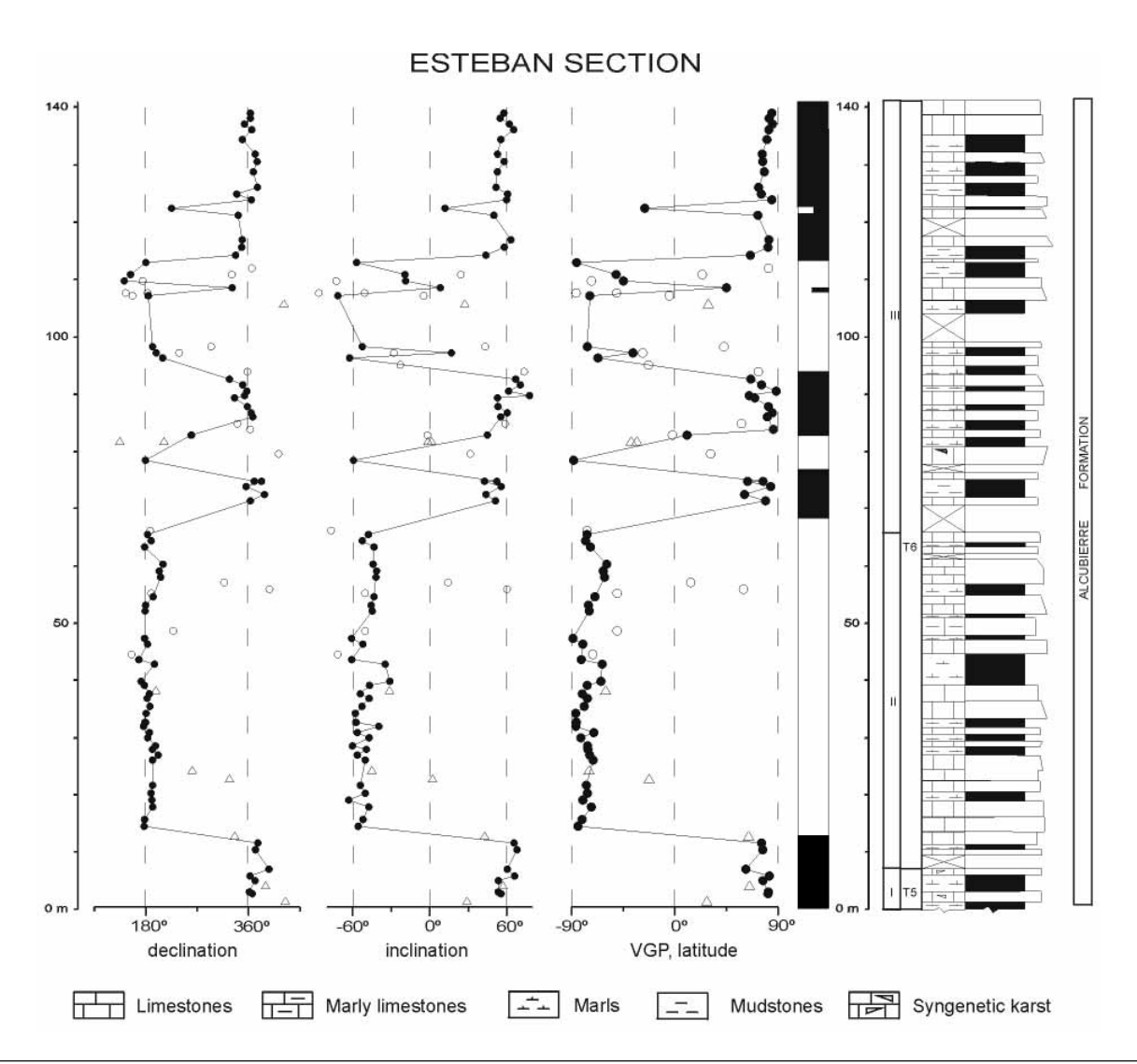


FIGURE 5 Stratigraphic column and magnetostratigraphy of the Esteban section. Solid dots represent highly reliable directions, open circles and triangles represent less reliable ones. Black (white) bands represent normal (reverse) polarity.

The passage to unit T6 is located at the top of this interval. The second part consists of beige, white, grey and yellow limestone, commonly grouped into thick sets of strata, and green and grey marls. Most limestones, particularly those at the lower third, correspond to laminated facies consisting of micrite with very thin intercalations of silt and fine sandstone laminae and lenticules. The rest are bioclastic and bioturbated facies. The third part of the section is made of alternating beige, brown and grey marls and limestones style. Most limestones correspond to structureless bioclastic and bioturbated facies. The uppermost part has thick bioturbated and nodulised limestone strata.

PALEOMAGNETIC RESULTS

The Castillo de Sora and Esteban sections (Figs. 4 and

5) were sampled at 1 meter intervals, obtaining a total of 196 sites. Two oriented cores per site were collected and 210 samples were analysed in order to obtain the local magnetic polarity stratigraphy. The studied lithologies consist of limestones, marly to sandy limestones, dolostones, marls and brown to red mudstones.

The Natural Remanent Magnetisation (NRM) was measured in a three-axes superconducting magnetometer and analysed using standard stepwise thermal (TH) demagnetisation procedures. A successful isolation of the paleomagnetic components was possible after treatment to 10 to 15 demagnetisation steps and up to 650°C. The visual inspection of Zijderveld plots revealed the presence of three components in most of the samples (Fig. 6). A randomly oriented small viscous component was removed at 100°C to 150°C. Above this temperature a

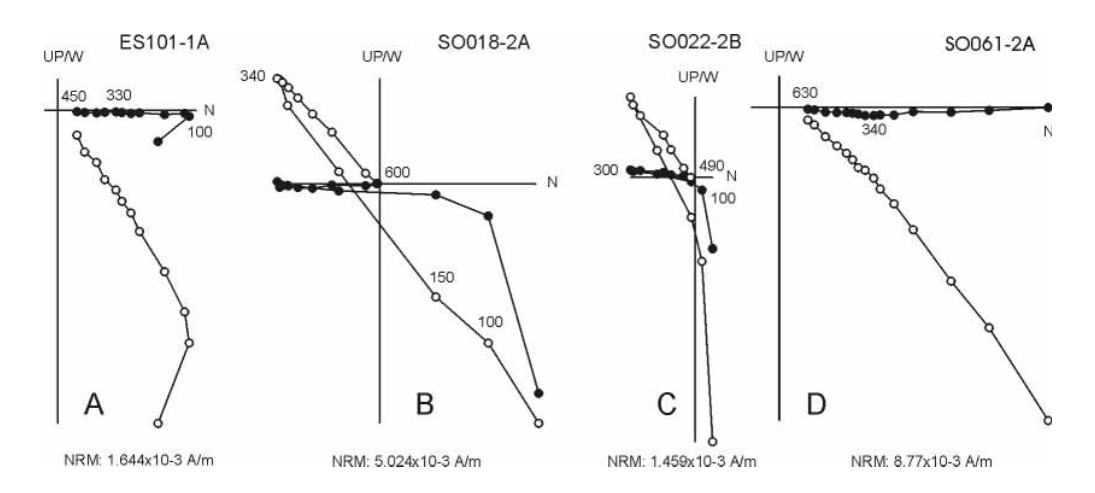


FIGURE 6 | Examples of thermic demagnetization diagrams from some samples of the studied sections. Solid (open) symbols are projections of vector endpoints onto the horizontal (vertical) plane. Numbers on the curve give temperatures in °C.

north directed component which parallels the present-day field represents a significant proportion of the remaining NRM. This secondary component is easily removed after treatment to 300°C-340°C. At higher temperatures a characteristic remanent magnetisation (ChRM) is isolated and shows both normal and reverse polarity. Demagnetisation of the ChRM yields a linear decay towards the origin with maximum unblocking temperatures ranging from 490°C to 630°C depending on the lithology. Complete demagnetisation at temperatures lower than 550°C-600°C is typically observed in limestones and grey marls, where the magnetite is the most likely magnetic carrier (Figs. 6A, 6B, 6C). Maximum unblocking temperatures above 630°C suggesting the presence of hematite are frequent in

the red mudstone intervals from the lower part of the Castillo de Sora section (Fig. 6D).

The occurrence of both magnetite and hematite in the studied sediments is further illustrated with the IRM data from a set of representative samples. Stepwise acquisition of the IRM up to 1 Tesla was combined with thermal demagnetisation of the IRM at 1 Tesla and 0.1 Tesla applied successively in two orthogonal directions (Lowrie, 1990). The shapes of the IRM acquisition curves (Fig. 7A) vary over a range which denotes the variable contributions of soft and hard magnetic minerals in the sampled sediments. Rapid IRM acquisition and saturation at fields below 0.2 T corresponds to magnetite bearing

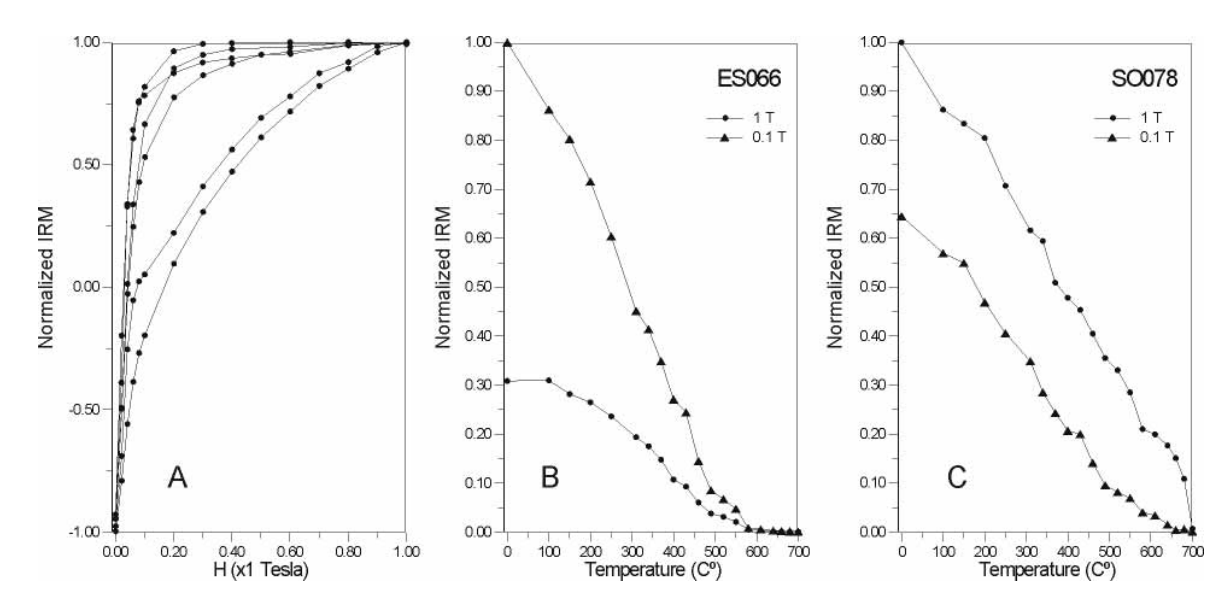


FIGURE 7 | IRM acquisition (A) and progressive demagnetization (B,C) of representative samples, both normalised. Castillo de Sora (SO) and Esteban (ES).

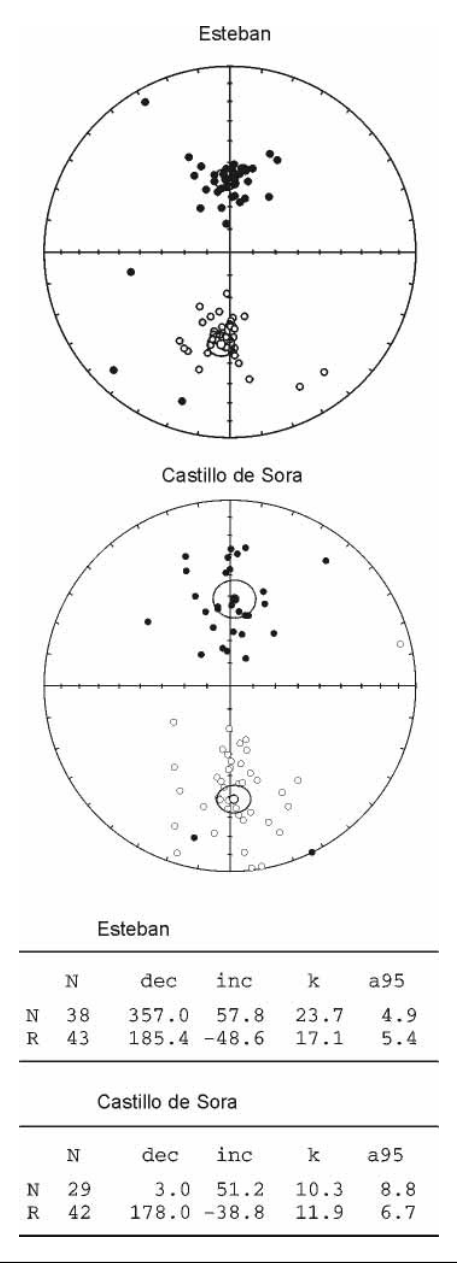


FIGURE 8 Equal-area stereographic projections of characteristic directions (normal and reverse polarities). Open (solid) symbols plotted on upper (lower) hemisphere

samples and show IRM unblocking temperatures of 580°C (Fig. 7B). Unsaturated samples at 1 Tesla show unblocking temperatures of the hard component of about 660°C (Fig. 7C), which is clear indication of hematite occurrence. In most of the cases samples show intermediate behaviour with occurrence of both magnetite and hematite in variable proportions.

The average normal and reverse components of the ChRM show nearly antipodal directions. Reverse directions show slightly shallower directions, which may result

from a partial overlap with the north directed low temperature component. The mean paleomagnetic declination (Fig. 8) is not significantly different from the reference geomagnetic field direction, therefore we can assume that no vertical axis rotation has occurred since deposition of the Montes de Castejón sediments.

CORRELATION WITH THE GPTS

The virtual geomagnetic pole (VGP) latitude calculated for each paleomagnetic site in both the Castillo de Sora and Esteban sections defines a sequence of seven magnetozones in each section. The stratigraphic correlation between both sections (Fig. 3) established by Arenas (1993) yielded an overlap of some tens of meters which is coherent with the magnetostratigraphic data from both sections (Fig. 9). The combined results provide a composite magnetic polarity sequence consisting of 12 magnetozones: 6 of reverse polarity (R1-R6) and 6 of normal polarity (N1-N6).

The correlation of the Montes de Castejón composite magnetostratigraphy with the Geomagnetic Polarity Time Scale (GPTS) of Cande and Kent (1995) can be established on the basis of the available chronostratigraphic constraints for equivalent sediments in the Ebro Basin (see Geological Context) and the distinctive pattern of local magnetozones. Assuming a coarse late Ramblian to early-middle Aragonian (early to middle Miocene) age for units T5 and T6, the long reverse interval (R4) with three shorter intervals below (N1-N2-N3) and two above (N4-N5) leaves correlation with the C5Br as the most probable. The triplet of normal magnetozones N1 to N3 in the Castillo de Sora section can be correlated with the characteristic triple chron C5C. Similarly, N4 to N6 in the upper Esteban section correlates with the two short chrons in C5Bn and the lower part of C5AD. As a result, the entire composite magnetostratigraphic succession of the Montes de Castejón ranges from C5Cr to C5ADn and spans approximately 2.6 Ma, from ~17 to ~14.3 Ma.

DISCUSSION

The previous magnetostratigraphic results from the Miocene sediments of the Sierra de Alcubierre (Pérez-Rivarés et al., 2002) provided an independent correlation with the GPTS. This study showed that at the T5/T6 boundary in the San Caprasio section, clearly defined by a rapid replacement of evaporite facies with carbonate facies, the local magnetostratigraphy apparently missed parts of chron C5Cn, yielding an uncertain dating of this TSU boundary (Fig. 9). On the other hand, in the Lanaja section where the magnetostratigraphy is more complete, the stratigraphic location of the T5/T6 boundary was

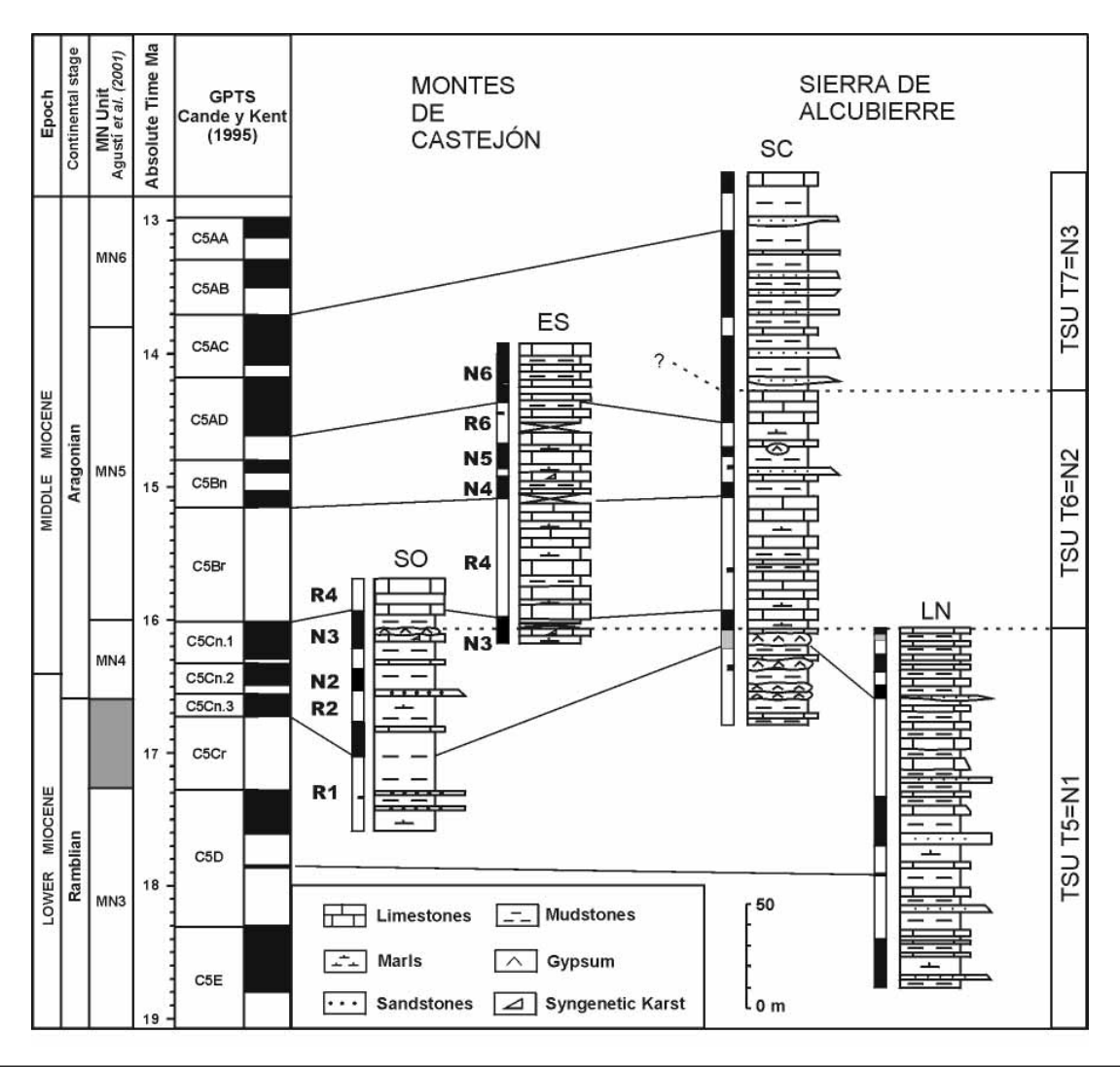


FIGURE 9 | Magnetostratigraphic correlation between the Montes de Castejón succession, Sierra de Alcubierre succession and the GPTS (Cande and Kent, 1995). Grey bands indicate the uncertain boundaries of biozones and chrons. TSU: Tectosedimentary units.

roughly placed by fotogeology methods within an interval of carbonate facies. From these data, the authors estimated the age of T5/T6 boundary at approximately 16.4 Ma (C5Cn.2n), based on the magnetostratigraphy of Lanaja.

Unlike the Sierra de Alcubierre, the magnetostratigraphy of the Montes de Castejón yields a complete record of chron C5Cn. Here, the stratigraphic location of T5/T6 boundary is determined in an evaporitic interval at the transition from the alluvial sediments of the Uncastillo Formation and the lacustrine limestones of the Alcubierre Formation (Figs. 3 and 4). It is also defined at the top of syngenetic karts layers within the Alcubierre Formation (Figs. 3 and 5). As shown above, this interval correlates with chron C5Cn.1n, with an interpolated age of about 16.14 Ma (Fig. 9), which is now assumed to be the best estimate for the T5/T6 boundary.

The correlation of the Montes de Castejón section with the GPTS allows an evaluation of the sedimentation rates through time. The Sora Section shows well determined magnetostratigraphic boundaries, which allow to estimate short-term sedimentation rates (calculated at the subchron level); these vary significantly from 6 to 26 cm/Ka. It must be noted, however, that errors of absolute ages in the GPTS should safely be taken in the range of 10⁴ years. This can be easily illustrated when comparing ages of the Astronomical Polarity Time Scale (APTS) with previous geomagnetic polarity time scales (Cande and Kent, 1992; 1995). For chrons shorter than 100 Ka, astronomical calibration has yielded durations that differ significantly from the radiometrically based GPTS (as much as 50% of their estimated duration) (Fig. 10). Therefore, sedimentation rates estimated over short periods (subchrons shorter than 100 Ka) must be taken with

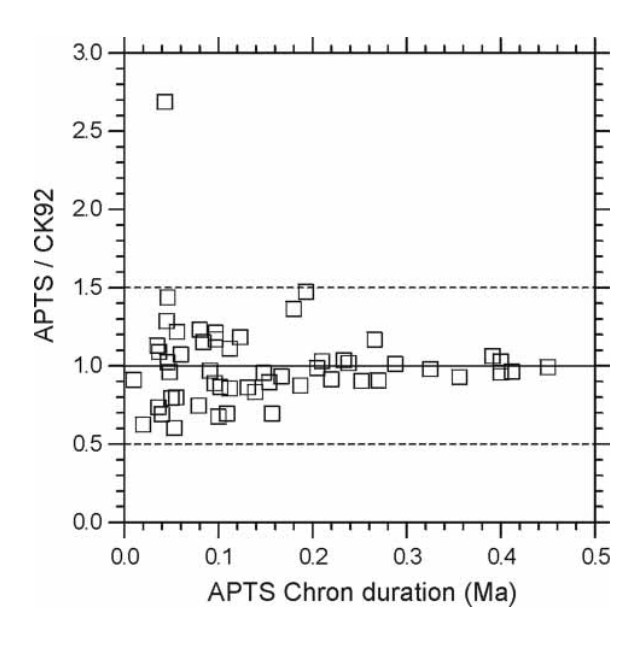


FIGURE 10 Values of APTS chron duration plotted against APTS/CK92 (GPTS after Cande and Kent, 1992) showing more pronounced differences in chron duration between astronomical calibration and radiometrically based calibration time scales for chrons shorter than 100 Ka.

caution unless an astronomical calibration is available. Still, it is remarkable the abrupt decrease in sedimentation occurring in chron C5Cn.1n, in coincidence with the observations in the San Caprasio section (Sierra de Alcubierre), where the same time slice records a significant hiatus of about 0.4 Ma (Pérez-Rivarés et al., 2002). This corresponds to the T5/T6 boundary, which represents an abrupt change from sulphate depositional environments (T5) to an expanding carbonate depositional lacustrine system (T6). Above the T5/T6 boundary the average sedimentation rates estimated in both the Montes de Castejón and Sierra de Alcubierre are not significantly different (8.85 cm/ka and 7.95 cm/Ka respectively). T6 in San Caprasio is about 115 m thick, similar to the 135 m measured in Esteban (Fig. 9). However, when compared the sediment thickness over a shorter time scale (at the subchron scale) the two areas show different trends. If the stratigraphic interval which correlates with chron C5Bn.1r is considered, in the San Caprasio section the sediment thickness (12 to 13.5 m) is about double compared to the Esteban section (3 to 7.5 m) (Fig. 11). In the Esteban section, this interval corresponds to bioclastic limestones affected by karstification, marls and mudstones (Arenas et al., 1999). The same time interval in the section of San Caprasio is represented by a sequence of mudstones, sands, sandstones and laminated sandy limestones. The next stratigraphic interval corresponding to chron C5Bn.1n shows that the relation between Esteban and San Caprasio is the opposite: a thick interval (10 to 13.5 m) of bioturbated bioclastic limestones alternating with marls in the Esteban section is equivalent

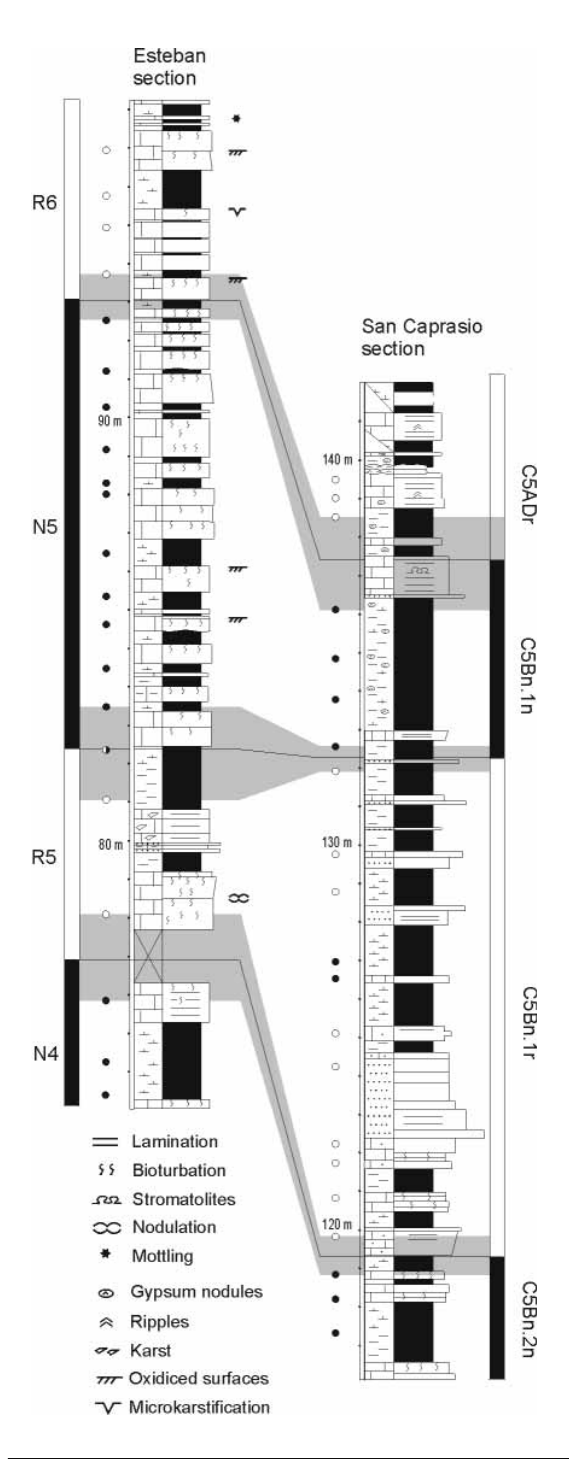


FIGURE 11 Detailed stratigraphy and magnetostratigraphy of the Esteban (Montes de Castejón) and San Caprasio (Sierra de Alcubierre) sections to show differences in thickness and facies of lacustrine deposits between these two areas. Solid (open) dots indicate position of the normal (reverse) polarity samples. Grey bands indicate the uncertainty polarity intervals.

in San Caprasio to a thin interval (4 to 6.5 m) of ochre mudstones, grey marls and some laminated limestones with abundant sulphate nodules.

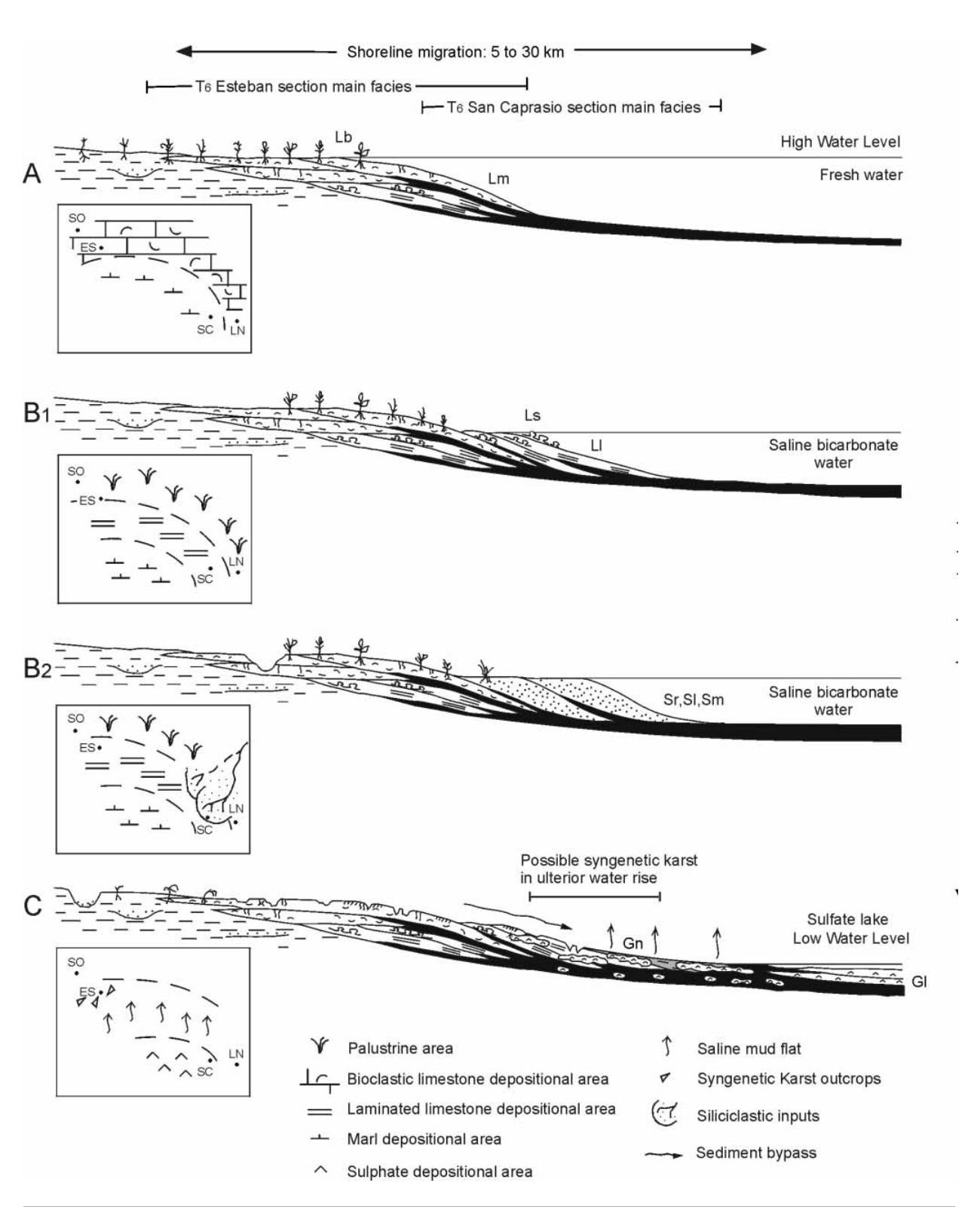


FIGURE 12 | Sedimentary facies model (modified from Arenas and Pardo, 1999) to explain the different sedimentary rates between Montes de Castejón and Sierra de Alcubierre successions. The scheme shows the different facies and processes resulting from a continuous fall of water level from freshwater (HWL) to saline, sulphate (LWL) depositional environments. Maps show the facies areal distribution correspondent to each water level case, with indication of the location of the sections. SO: Castillo de Sora; ES: Esteban; SC: San Caprasio; LN: Lanaja. Gn: nodular gypsum; Gl: laminated gypsum; LI: laminated limestones and dolostones; Ls: stromatolitic limestones and dolostones; Lm: massive limestones; Lb: bioturbated limestones; Sm: masive sandstones; SI: laminated sandstones; Sr: rippled sandstones.

The contrasting facies and sediment thickness observed between Montes de Castejón and San Caprasio can be related to the different sedimentary locations within the proposed sedimentary lacustrine model (Arenas and Pardo, 1999), and were ultimately controlled by the cyclic water level fluctuations that experienced the lacustrine system (Fig. 12). During periods of high water level (Fig. 12A) there was a single water body in which freshwater carbonate depositional conditions prevailed, giving rise to thick layers of bioclastic limestone facies on the outer fringes of the lake (Esteban section), while thinner layers of marls were deposited in offshore areas (San Caprasio). At the same time the Sora area recorded mostly distal alluvial sedimentation. Episodic lowering of the water level (Fig. 12B1) led to exposure ancient carbonate areas, which became palustrine fringes, while in the lake more saline carbonate facies (laminated limestones and stromatolites) formed on the littoral fringes and marl deposition continued offshore. By the time of extreme low water levels (Fig. 12C), the littoral carbonate and marl facies were exposed, undergoing syndepositional saline diagenetic processes (e.g., cracks, breccia, growth of sulphate nodules and pseudomorphs), while sulphate precipitation occurred in the lake water. Subsequent water level rises led the previous syndepositional saline diagenetic products to suffer dissolution and new precipitations processes; it was then when the syngenetic karts facies finalized its features. Alternating high and low water levels gave rise to simple sequences, dm to m thick, described by Arenas and Pardo (1999).

According to this model, the upper part of T5 probably recorded some of the lowest and more prolonged periods of low water levels in the basin, causing exposition of large lacustrine areas. A condensed lacustrine sedimentation at the end of T5 in the central parts of the basin could be coherent with repeated long periods of extreme aridity and low water levels. At the same time span, in high water level periods, subaerial areas directly connected with the main fluvial system (Luna System), such as the Castillo de Sora area, could keep moderate accumulation rates as a consequence of terrigenous sediment supply. The variable sedimentation rates through C5Cn (6 to 26 cm/ka) could be partly interpreted as the result of the unsteady and discontinuous character of these depositional systems. But as noted above, this variable short-term sedimentation rates are subjected to the uncertainties of the time scale that can be larger than the inferred fluctuations in sedimentation when very short subchrons are considered.

Another period of dominant low water levels corresponded to magnetozone R5 (Fig. 11) causing exposition of the carbonate fringes and syngenetic karstification in the Esteban section. At the same time, the decreasing accommodation space along the margins propitiated sedi-

ment bypass and progradation of detrital wedges towards the inner parts of the basin (San Caprasio area, Fig. 12B2). These localised terrigenous contributions were responsible for the relatively high sedimentation rates in San Caprasio associated to R5 (Fig. 11). A period of dominantly high water levels is best represented during N5 (Fig. 11), when the Esteban section records thick packages of bioclastic limestones. Increased accommodation along the fringing areas facilitated the aggradation of these units while in the inner parts of the lake (San Caprasio), deposition of condensed marly sequences occurred. Briefly, during the time of magnetozones R5 and N5 the San Caprasio area recorded sedimentation that corresponded mostly to inner lacustrine parts, with continuous and low rate sedimentation, excepting the case of episodic detrital inputs. At the same time, the Esteban sector remained mostly as outer carbonate fringes, in which sedimentation was less continuous, with common hiatuses, but with higher rates at times of high water level.

CONCLUSIONS

The paleomagnetic analysis of the Miocene sedimentary record of the Montes de Castejón, which covers the upper part of TSU T5 and TSU T6, indicates that the natural remanent magnetization is carried by magnetite and hematites, and reveals a composite magnetic polarity of 12 magnetozones. The local magnetostratigraphy can be independently correlated with the GPTS (chrons C5Cr to C5ADn).

In the central sector of the Ebro Basin the boundary between units T5 and T6 is present in both the Montes de Castejón and the Sierra de Alcubierre successions. The magnetostratigraphy of the Montes de Castejón allows a best estimate of 16.14 Ma for the age of T5/T6 boundary (within chron C5Cn.1n).

Accurate correlation through the central sector of the Ebro Basin based on magnetostratigraphy shows thickness and facies differences between distant areas of the basin at particular time intervals (e.g., Esteban section in the Montes de Castejón and San Caprasio section in the Sierra de Alcubierre). The sedimentary facies model proposed for the late Oligocene-Miocene lacustrine system (Arenas and Pardo, 1999) explains that during chrons C5Cn to C5Bn.1n these two areas occupied different sedimentary positions within a lacustrine system that experienced cyclic water level fluctuations through time. During the deposition of unit T6 the San Caprasio area mostly corresponded to offshore areas with continuous and steady sedimentation rates. In contrast, the Esteban area mostly corresponded to outer carbonate fringes, with discontinuous and unsteady sedimentation caused by the lake level fluctuations: high sedimentation rates at times of high water level and hiatuses at times of low water level.

ACKNOWLEDGEMENTS

We thank the Laboratori de Paleomagnetisme de Barcelona (Instituto de Ciencias de la Tierra "Jaume Almera", UB-CIRIT-CSIC), where the analyses were carried out. This research was funded by project PB97-0882-C03 of the DGES (Technology and Science Ministry of Spain) and forms part of the objectives of the group "Continental sedimentary basin analysis" of the Aragón Government (Spain). We thank Drs. J. Villalain and W. Krijgsman for their helpful comments and suggestions of the manuscript.

REFERENCES

- Alonso-Zarza, A.M., Armenteros, A., Braga, J.C., Muñoz, A., Pujalte, V., Ramos, E., Aguirre, J., Alonso-Gavilán, G., Arenas, C., Baceta, J.I., Carballeria, J., Calvo, J.P., Corrochano, A., Fornós, J.J., González, A., Luzón, A., Martín, J.M., Pardo, G., Payros, A., Pérez, A., Pomar, L., Rodríguez, J.M., Villena, J., 2002. Tertiary. In: Gibbons, W., Moreno, T. (eds.). The Geology of Spain. London, Geological Society, 293-334.
- Arenas, C., 1993. Sedimentología y paleogeografía del Terciario del margen pirenaico y sector central de la Cuenca del Ebro (zona aragonesa occidental). Doctoral thesis, Universidad de Zaragoza, 858 pp.
- Arenas, C., Pardo, G., 1999. Latest Oligocene-late Miocene lacustrine systems of the north-central part of the Ebro Basin (Spain): sedimentary facies model and palaeogeographic synthesis. Palaeogeography Palaeoclimatology Palaeoecology, 151, 127-148.
- Arenas, C., Alonso Zarza, A.M., Pardo, G., 1999. Dedolomitizacion and other early diagenetic processes in Miocene lacustrine deposits, Ebro Basin (Spain). Sedimentary Geology, 125, 23-45.
- Arenas, C., Pardo, G., 2000. Neogene lacustrine deposits of the north-central Ebro Basin, northeastern Spain. In: Gierlowski-Kordesch, E.H., Kelts, K.R. (eds.). Lake basins through space and time. American Association of Petroleum Geologists, Studies in Geology, 46, 395-406.
- Barberà, X., Cabrera, L., Marzo, M., Parés, J.M., Agustí, J., 2001. A complete terrestrial Oligocene magnetobiostratigraphy from the Ebro Basin, Spain. Earth and Planetary Science Letters, 187, 1-16.
- Cande, S., Kent, D., 1992. A new geomagnetic polarity timescale for the Late Cretaceous and Cenozoic. Journal of Geophysical Research, 97, 13917-13951.
- Cande, S., Kent, D., 1995. Revised calibration of the Geomagnetic Polarity Time Scale for the late Cretaceous and Cenozoic. Journal Geophysical Research, 100, 6093-6095.
- Cuenca, G., Canudo, J.I., Laplana, C., Andrés, J.A., 1992. Bio y cronoestratigrafía con mamíferos en la Cuenca Terciaria del Ebro: ensayo de síntesis. Acta Geologica Hispanica, 27(1-2), 127-143.
- García-Castellanos, D., Vergés, J., Gaspar-Escribano, J., Cloet-

- ingh, S., 2003. Interplay between tectonics, climate and fluvial transport during the Cenozoic evolution of the Ebro Basin (NE Iberia). Journal Geophysical Research, 108, B7, 2357, doi:10.1029/2002JB002073.
- Gomis, E., Parés, J.M., Cabrera, L., 1997. Nuevos datos magnetoestratigráficos del tránsito Oligoceno-Mioceno en el sector SE de la Cuenca del Ebro (provincias de Lleida, Zaragoza y Huesca, NE de España). Acta Geologica Hispanica, 32, 185-199
- Hirst, J.P.P., Nichols, G.J., 1986. Thrust tectonic controls on Miocene alluvial distribution patterns, southern Pyrenees.
 In: Allen, P.A., Homewood, P. (eds.). Foreland Basins, International Association Sedimentologists, Special Publication 8, 247-258.
- Instituto Tecnológico y Geominero de España, 1995. Mapa Geológico de la Península Ibérica, Baleares y Canarias. Scale 1:1.000.000, Madrid.
- Lowrie, W., 1990. Identification of ferromagnetic minerals in a rock by coercivity and unblocking temperature properties. Geophysics Research Letters, 17, 159-162.
- Odin, G.S., Cuenca, G., Canudo, J.L., Cosca, M., Lago, M., 1997. Biostratigraphy and geochronology of a Miocene continental volcaniclastic layer from the Ebro basin, Spain. In: Montanary, A., Odin, G.S., Coccioni, R. (eds.). Miocene Stratigraphy: An Integrated Approach. Amsterdam, Elsevier Science B.V., 297-310.
- Pardo, G., Villena, J., González, A., 1989. Contribución a los conceptos y a la aplicación del análisis tectosedimentario. Rupturas y unidades tectosedimentarias como fundamento de correlaciones estratigráficas. In: Vera, J.A. (ed.). División de unidades estratigráficas en el análisis de cuencas. Revista Sociedad Geológica de España, 2, 199-221.
- Pérez, A., Azanza, B, Cuenca, G., Pardo, G., Villena, J., 1985. Nuevos datos estratigráficos y paleontológicos sobre el Terciario del borde meridional de la depresión del Ebro (provincia de Zaragoza). Estudios Geológicos, 41, 405-411.
- Pérez-Rivarés, F.J., Garcés, M., Arenas, C., Pardo, G., 2002. Magnetocronología de la sucesión miocena de la Sierra de Alcubierre (sector central de la Cuenca del Ebro). Revista Sociedad Geológica de España, 15, 210-225.
- Quirantes, J., 1978. Estudio sedimentológico y estratigráfico del Terciario continental de Los Monegros. Zaragoza, ed. Institución Fernando El Católico (C.S.I.C.), Diputación Provincial de Zaragoza, 200 pp.
- Riba, O., Reguant, S., Villena, J., 1983. Ensayo de síntesis estratigráfica y evolutiva de la cuenca terciaria del Ebro. In: Comba, J.A. (coord.). Geología de España, Libro Jubilar J.M. Ríos. Madrid, Instituto Geológico y Minero de España, 131-159.
- Soler, M., Puigdefábregas, C., 1970. Líneas generales de la geología del Alto Aragón Occidental. Pirineos, 96, 5-20.
- Vázquez-Urbez, M., Arenas, C., Pardo, G., 2003. Facies fluviolacustres de la unidad superior de la Muela de Borja (Cuenca del Ebro): Modelo sedimentario. Revista Sociedad Geológica de España, 15, 41-54.

Villena, J., González, A., Muñoz, A., Pardo, G., Pérez, A., 1992. Síntesis estratigráfica del Teciario del borde Sur de la Cuenca del Ebro: unidades genéticas. Acta Geologica Hispanica, 27(1-2), 225-245.

Villena, J., Pardo, G., Pérez, A., Muñoz, A., González, A.

1996. The Tertiary of the Iberian margin of the Ebro basin: sequence stratigraphy. In: Friend, P.F., Dabrio, C.J. (eds.). Tertiary basins of Spain: the stratigraphic record of crustal kinematics. Cambridge, Cambridge University Press, 77-82.

Manuscript received october 2003; revision accepted April 2004.